Published in Applied Physics Letters 73, 2158-2160, 1998
which should be used for any reference to this work

Room-temperature pulsed operation of an electrically injected InGaN/GaN multi-quantum well distributed feedback laser

Daniel Hofstetter,[a] Robert L. Thornton,[b] Linda T. Romano, David P. Bour, Michael Kneissl, and Rose M. Donaldson
Xerox Palo Alto Research Center, 3333 Coyote Hill Road, Palo Alto, California 94304

We demonstrate room-temperature pulsed operation of an electrically injected InGaN/GaN-based distributed feedback laser with an emission wavelength of 403 nm. The threshold current of a 1000-μm-long and 20-μm-wide device was 3.2 A; corresponding to a threshold current density of 16 kA/cm^2. The 3rd order grating providing feedback was defined holographically and dry etched into the upper waveguiding layer by chemically assisted ion beam etching. We observed single mode operation of the laser with a side mode suppression ratio of 15 dB over a temperature range of about 30 K.

The development of an electrically pumped laser emitting light around 400 nm has experienced tremendous progress during the past couple of years. Under the lead of Nakamura *et al.* both pulsed and continuous wave operation of InGaN/GaN based devices have been demonstrated at room temperature.[1–4] One of the main concerns in nitride lasers is the fabrication of high quality mirrors. While the lattice misorientation to sapphire substrates makes cleaved facet devices difficult to realize, sawing and subsequent polishing of the laser mirrors is a very time-consuming process. Dry-etched mirrors with high reflective coatings seem to work well in this material system.[5] However, when growing on sapphire substrates, these etched mirrors are typically not at the edge of the substrate. Thus, usually a certain fraction of the optical mode gets diffracted into or reflected from the sapphire surface, leading to an asymmetric far field with multiple emission lobes in the vertical direction.[1,6] The use of distributed feedback for providing optical cavity formation could partly eliminate some of the mirror issues because no optical quality mirrors are required to achieve lasing action. Moreover, the longitudinal mode structure, which, due to the close mode spacing in these devices, is very competitive and noisy, could be markedly improved by using the distributed feedback (DFB) mechanism for mode selection. This idea has already been explored to some extent by the fabrication of optically pumped DFB lasers. Very narrow linewidths, locking of the emission wavelength to the grating resonance wavelength, and operation even at the absence of cavity mirrors have been reported for such optically pumped devices.[7,8]

In this article, we demonstrate the fabrication of an electrically injected InGaN/GaN-based DFB laser with a holographically defined 3rd order grating. When compared to normal Fabry–Perot devices fabricated from the same material, we observe a comparable threshold current density, single mode behavior with a higher side mode suppression ratio, and a modehop-free tuning over a temperature range of more than 30 K. This guarantees a reduced temperature sensitivity of the lasing wavelength relative to Fabry–Perot lasers.

The fabrication of these devices relied on growing a 4-μm-thick *n*-type GaN:Si layer on *C*-face sapphire. On top of this layer, we grew a 500-nm-thick, *n*-doped $Al_{0.08}Ga_{0.92}N$:Si lower cladding layer, a 100-nm-thick *n*-doped GaN:Si lower waveguiding layer, a 30-nm-thick undoped active region with five 3-nm-thick $In_{0.15}Ga_{0.85}N$ quantum wells and 7-nm-thick GaN barriers, and a 180-nm-thick *p*-doped GaN:Mg upper waveguiding layer. The 3rd order grating with a period of 240 nm was then defined by a holographic exposure and dry etched into the upper waveguiding layer by chemically assisted ion beam etching. The grating depth was nearly 100 nm, which results in a high coupling coefficient of 100 cm^{-1} for a rectangular grating. However, since the tooth shape of the grating was not perfectly rectangular, the coupling coefficient was reduced to the order of 5–10 cm^{-1}. For a cavity length of 1000 μm, this coupling strength would roughly translate into an effective reflectance of 15%–30%. Figure 1 shows an atomic force microscopy (AFM) surface scan of the grating before regrowth. A root mean square (rms) surface roughness of around 3–5 nm was observed; this is comparable to the rms roughness of the as-grown surface. After grating fabrication, we performed optical pumping experiments in order to confirm the matching between the grating resonance wavelength and the gain peak. Then, we pro-

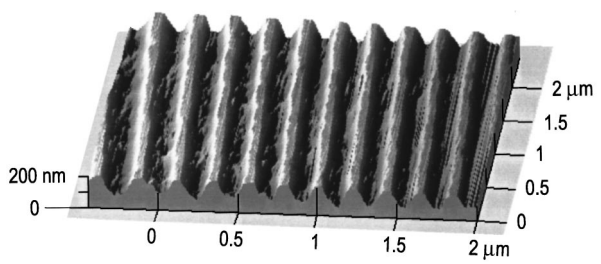

FIG. 1. AFM surface scan of a 3rd order diffraction grating in GaN before over growing the upper cladding and the contact layer.

[a]Now with: Institute of Physics, University of Neuchâtel, Rue A.-L. Breguet 1, 200 Neuchâtel, Switzerland.
Electronic mail: Daniel.Hofstetter@iph.unine.ch
[b]Now with: Maxtek Components Corporation, 13335 SW Terman Road, Beaverton, Oregon 97075-0428.

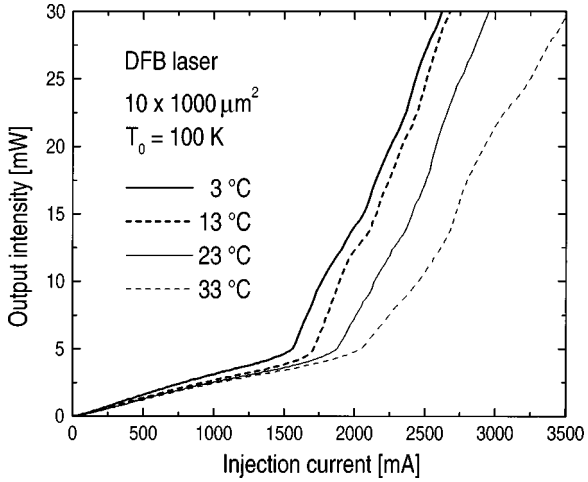

FIG. 2. $L-I$ characteristics of an InGaN/GaN DFB laser with an active area of 10×1000 μm^2 at four different heat-sink temperatures.

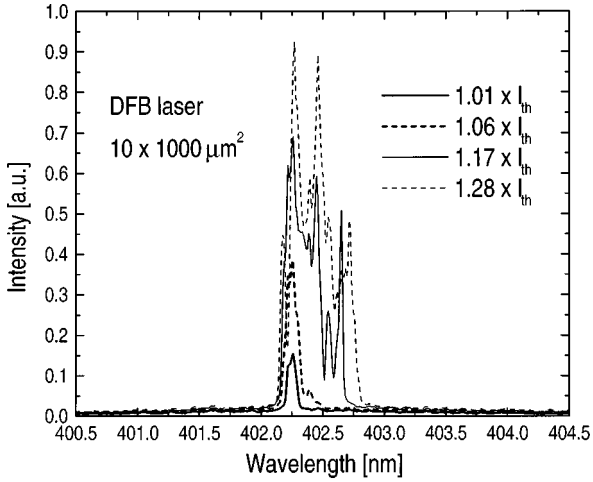

FIG. 3. Emission spectra of an InGaN/GaN DFB laser at four different injection current levels ranging from $1.01\times I_{\rm th}$ to $1.28\times I_{\rm th}$. All curves are drawn using the same vertical scale.

ceeded with an epitaxial regrowth to complete the device structure. This regrowth consisted of a 300-nm-thick *p*-doped $Al_{0.08}Ga_{0.92}N$:Mg upper cladding layer and a 100-nm-thick *p*-type GaN:Mg contact layer. Cross-sectional transmission electron microscope studies of the overgrown grating showed that no additional dislocations were created at the interface between the grooved GaN waveguide layer and the upper AlGaN cladding layer. This observation is in sharp contrast to InGaAsP/InP-based infrared DFB lasers, where the grooved interface serves as starting point for numerous dislocations.[9]

Device processing involved the definition of mesas to enable lateral *n* type contacting of the devices, and evaporation of standard *n*- and *p*-metal Ti/Au layers. The *p*-metal contact stripes were 4, 10, or 20 μm wide, and thus defined the width of the gain region. A SiON layer was used to electrically isolate the noncontacted areas and the sidewalls of the mesas, thereby restricting gain to within a narrow stripe in the lateral direction. Following the SiON window etch, we evaporated another Ti/Au layer in order to provide the *p*-metal contact pads for the probe. Finally the mirrors were etched, again by chemically assisted ion beam etching. In order to ensure that these lasers would not accidentally oscillate as Fabry–Perot lasers, we dry etched only one of the facets exactly vertical while leaving the other one at an angle of approximately 20° to the vertical. As a result of this fabrication procedure, we obtained gain guided DFB lasers with cavity lengths of up to 1000 μm and stripe widths of 4, 10, and 20 μm.

Measurements of the current–voltage ($I-V$) and light output-current ($L-I$) characteristics were carried out under pulsed current conditions (500 ns pulse length, 0.05% duty cycle) at room temperature. The lasers were probe contacted and tested on chip. At 1 mA forward current, the $I-V$ curve typically exhibited a ''turn on voltage'' of 3.3 V, and for a 10×1000 μm^2 contact region, we observed a series resistance of 10 Ω. As shown in the $L-I$ curves of Fig. 2, we obtained, for the longest devices with 10 μm stripe width, pulsed threshold currents of 1550 mA at 3 °C and 2050 mA at 33 °C. From these measurements, we determine the T_0 value to be approximately 100 K. A value of $T_0=150$ K was found for Fabry–Perot type lasers fabricated from the same material. The stronger temperature dependence of the DFB laser's threshold current can be explained by the different T-tuning coefficients of the gain peak and the grating resonance peak, which, at elevated temperatures, lead to an increasing mismatch between the maximal reflectance peak of the grating and the gain maximum.

The best threshold currents were obtained on lasers with 20 μm stripe width and 1000 μm cavity length. Values of 3200 mA for 20 μm-wide devices were observed, corresponding to threshold current densities of 16 kA/cm^2. For shorter (500 μm long) devices with 20 μm stripe width, we measured higher threshold currents of 4600 mA (threshold current density of 23 kA/cm^2). For the best devices, typical threshold voltages of $V(I_{\rm th})=16$ V were seen.

High-resolution spectra of these lasers were measured using a grating spectrometer with a resolution of 0.5 Å (SPEX, $d_{\rm focal}=1.26$ m, $w_{\rm slit}=50\mu m$). The laser output was focused on to a quartz fiber using a microscope objective, and fed into the input slit of the spectrometer. By placing a 1024 element array photodetector into the output image plane, we were able to measure the spectrum in a spectral window of 10 nm width within 1 sec.

In Fig. 3, we show high-resolution emission spectra at various current levels ranging from $1.01\times I_{\rm th}$ to $1.28\times I_{\rm th}$. While there is only one clean peak with a resolution limited width of 0.5 Å for lower injection currents, there appear to be multiple peaks with an overall width of 5 Å at higher injection levels. The fact that all additional features occurred at the long wavelength side of the main peak suggests that chirping due to device heating during the current pulse could be responsible for this kind of broadening. From the spectral broadening at higher injection currents and the temperature tuning coefficient derived in the following paragraph, we were able to estimate the temperature increase during the pulse to be on the order of 20–30 K. Another possible reason for the spectral broadening at higher current levels is the onset of lasing in higher order lateral modes in these gain-guided structures. This explanation is supported by the fact that the $L-I$ curves show several kinks.

Emission spectra of a 1000-μm-long DFB laser at four different heat-sink temperatures are shown in Fig. 4; they

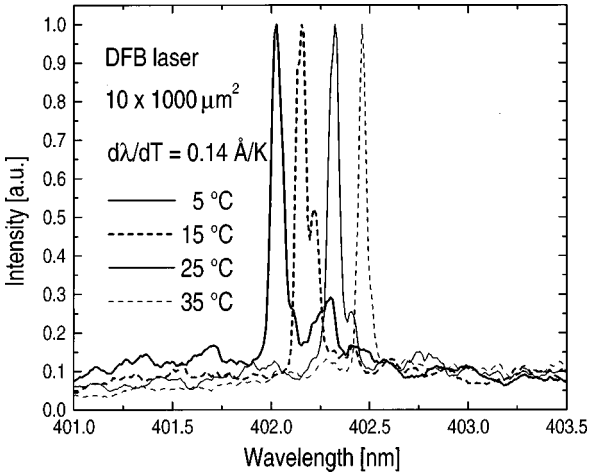

FIG. 4. Emission spectra of the same device as in Fig. 3 at $1.1\times I_{\text{th}}$ and at different heat-sink temperatures. The temperature tuning coefficient obtained was 0.14 Å/K.

reveal laser oscillation in a single longitudinal mode with a side mode suppression ratio of 15 dB and at a center wavelength of around 403 nm. Given the grating period of 240 nm and the above emission wavelength, we were able to calculate the effective refractive index of the propagating mode to be $n_{\text{eff}}=2.52$. In order to maintain narrow emission spectra for this measurement, we adjusted the injection current to always be at $1.1\times I_{\text{th}}$. The device remained in a single mode for temperatures ranging from 2 to 35 °C, which is a temperature range of more than 30 K; the temperature tuning coefficient was on the order of 0.014 nm/K. For Fabry–Perot type lasers fabricated on the same wafer, we measured a much larger average temperature tuning coefficient of 0.065 nm/K.

The far field of the DFB lasers reported in this article exhibits the usual interference effects due to the reflection from and the diffraction into the sapphire substrate. However, in the lateral direction, we observed a far field angle of approximately 10° above threshold, and a broad Lambertian characteristics below threshold. On Fabry–Perot lasers from similar material, we polished one mirror facet in order to get a far field measurement without the diffraction and refraction artifacts. Due to the insufficiently thick Al/GaN lower cladding layer, the result of this measurement was very similar to what we reported earlier on optically pumped lasers.[6] It revealed two main emission lobes in the vertical direction and a number of weaker oscillations in between.

In conclusion, we have demonstrated an electrically injected InGaN/GaN-based DFB laser. The best threshold current density observed was comparable to that of conventional Fabry–Perot type devices, and was on the order of 16 kA/cm^2. The T_0 value describing the T dependence of the threshold current was approximately 100 K. The reason for the much better T_0 value measured on Fabry–Perot devices fabricated from the same material ($T_0=150$ K) is the increasing mismatch between the grating resonance wavelength and the gain maximum when heating or cooling the DFB lasers. The emission of the DFB laser was at a wavelength of 403 nm and occurred in a single longitudinal mode with a side mode suppression ratio of 15 dB. The primary emission peak could be temperature tuned continuously between 2 and 35 °C at a rate of 0.14 Å/K.

The authors would like to thank Fred Endicott and Clarence Dunnrowicz for technical assistance, and Noble M. Johnson, Ross Bringans, Gary A. Evans (Southern Methodist University, Dallas, TX), and Peter S. Zory (University of Florida, Gainesville, FL) for helpful discussions. This work was supported by the Defense Advanced Research Projects Agency (DARPA Contract No. MDA 972-96-3-0014), and the Swiss National Science Foundation.

[1] S. Nakamura, M. Senoh, S. Nagahama, N. Iwasa, T. Yamada, T. Matsushita, Y. Sugimoto, and H. Kiyoku, Jpn. J. Appl. Phys., Part 2 **35**, L74 (1996).
[2] S. Nakamura, M. Senoh, S. Nagahama, N. Iwasa, T. Yamada, T. Matsushita, Y. Sugimoto, and H. Kiyoku, Appl. Phys. Lett. **69**, 1477 (1996).
[3] S. Nakamura, M. Senoh, S. Nagahama, N. Iwasa, T. Yamada, T. Matsushita, Y. Sugimoto, and H. Kiyoku, Appl. Phys. Lett. **72**, 211 (1998).
[4] D. P. Bour, H. F. Chung, W. Götz, B. S. Krusor, D. Hofstetter, S. Rudaz, C. P. Kuo, F. A. Ponce, M. G. Craford, and R. D. Bringans, in *Proceedings of the MRS 1996 Fall Meeting*, edited by F. A. Ponce, T. D. Moustakas, I. Akasaki, and B. A. Monemar (Materials Research Society, Pittsburgh, PA, 1996), Vol. 449, pp. 509–514.
[5] M. Kneissl, D. P. Bour, N. M. Johnson, L. T. Romano, B. S. Krusor, R. Donaldson, J. Walker, and C. Dunnrowicz, Appl. Phys. Lett. **72**, 1539 (1998).
[6] D. Hofstetter, D. P. Bour, R. L. Thornton, and N. M. Johnson, Appl. Phys. Lett. **70**, 1650 (1997).
[7] D. Hofstetter, R. L. Thornton, M. Kneissl, D. P. Bour, and C. Dunnrowicz, Appl. Phys. Lett. **73**, 1928 (1998).
[8] R. Hofmann, H.-P. Gauggel, U. A. Griesinger, H. Gräbeldinger, F. Adler, P. Ernst, H. Bolay, V. Härle, F. Scholz, H. Schweizer, and M. H. Pilkuhn, Appl. Phys. Lett. **69**, 2068 (1996).
[9] S. N. G. Chu, T. Tanbun-Ek, R. A. Logan, J. Vandenberg, P. F. Sciortino, Jr., P. Wisk, and T. L. Pernell, IEEE J. Sel. Top. Quantum Electron. **3**, 862 (1997).